Interface transparency of superconductor/ferromagnetic multilayers

J. Aarts and J. M. E. Geers
Kamerlingh Onnes Laboratory, Leiden University, P.O. Box 9506, 2300 RA Leiden, the Netherlands

E. Brück
van der Waals-Zeeman Laboratory, University of Amsterdam, Plantage Muidergracht 4, NL-1018 TV Amsterdam, the Netherlands

A. A. Golubov*
Institute of Solid State Physics, Chernogolovka, Moscow District, 142432, Russia

R. Coehoorn
Philips Research Laboratories, Prof. Holstlaan 4, 5656 AA Eindhoven, the Netherlands

(Received 5 March 1997)

We have investigated the behavior of the superconducting transition temperature T_c in superconducting/ferromagnetic (S/F) multilayers, as a function of the different layer thicknesses and for varying magnetic moment μ_F of the F-layer atoms. The system studied consists of superconducting V and ferromagnetic $V_{1-x}Fe_x$ alloys with x such that μ_F on the Fe atom is varied between 2 and $0.25\mu_B$. We determined the superconducting coherence length in the F layer ξ_F, which is found to be inversely proportional to μ_F. We also determined the critical thickness of the S layer, above which superconductivity appears. This thickness is found to be strongly nonmonotonic as function of the Fe concentration in the alloys. By analyzing the data in terms of the proximity-effect theory, we show that with increasing μ_F, the increasing pair breaking in the F layer by the exchange field is counteracted by a decreasing transparency of the S/F interface for Cooper pairs. [S0163-1829(97)02129-2]

I. INTRODUCTION

In combining a superconductor (S) with a ferromagnet (F) rather than with a normal metal, various effects have been predicted to occur. One is the modification of Andreev reflections at the S/F interface,[1] which would introduce spin selectivity in the conductance of an SF junction, with strong implications for devices at mesoscopic length scales.[2] Another is the possibility of a phase difference $\Delta\phi = \pi$ over an S/F/S junction,[3] resulting in an oscillatory behavior of the superconducting transition temperature T_c with F-layer thickness d_F of S/F multilayers.[4–6] An oscillation in T_c was recently reported for Nb/Gd,[7] but its origin is still controversial.[8] All such effects concern the behavior of the superconducting order parameter near the S/F interface, and in that sense they form part of the general issue of the proximity effect, well known for the S/N case, but hardly investigated for the S/F case. Apart from the spin dependence, the main parameter which discerns an F metal from an N metal in the framework of the proximity effect is the coherence length ξ_F, which measures the penetration depth of a Cooper pair into the ferromagnet. This length is supposed to be small, as can be estimated from the simple clean-limit expression

$$\xi_F = \hbar v_F / \Delta E_{\mathrm{ex}}. \tag{1}$$

With v_F a typical Fermi velocity of 10^6 m/s and ΔE_{ex} a typical exchange splitting of 1 eV, ξ_F is of the order of 1 nm, much smaller than the typical superconducting coherence length $\xi_S \approx 10$ nm. In consequence, the F layer thickness d^F_{dc}, needed to decouple two S layers (meaning that the order parameter in F is fully depressed), is very small. Furthermore, the order parameter on the S side will be profoundly influenced, since it must bend almost to zero at the interface. Experimentally, this translates into the fact that one S layer between two F layers needs a minimum or critical thickness d^S_{cr} for superconductivity to develop, d^S_{cr} being governed by both ξ_S and ξ_F. Of course, the concept of a critical thickness is not peculiar to the S/F problem. In S/N systems it may be encountered as well, but the behavior of T_c with d_S is more complicated because of the temperature dependence of the coherence length in the normal metal ξ_N. In the S/F case, the exchange energy is much larger than the superconducting transition temperature, which makes ξ_F virtually temperature independent. We will come back to this below.

Going one step further, it may be asked how ξ_F can be varied. Control is clearly by the exchange splitting ΔE_{ex}, defined as the effective energy difference for electrons at the Fermi level with spins parallel and antiparallel to the magnetization. It is connected to the magnetic moment μ_F of the host ion by

$$\Delta E_{\mathrm{ex}} = I_{\mathrm{eff}} \mu_F, \tag{2}$$

with I_{eff} an effective exchange integral. Thus, it is to be expected that ξ_F can be increased by lowering μ_F. Surprisingly, these simple concepts have never yet been investigated. It is the purpose of this paper to report such systematic research, and to show that the above-sketched picture misses one essential ingredient, namely the transparency of the S/F interface for Cooper pairs. We present measurements on S/F

TABLE I. Experimental values of the Fe moment μ_F, the magnetically dead layer $d_{\rm md}$, the decoupling thickness $d^F_{\rm dc}$, the critical thickness $d^S_{\rm cr}$, and the specific resistivity ρ at 6 K for alloys $V_{1-x}Fe_x$.

x	μ_F (μ_B)	$d_{\rm md}$ (nm)	$d^F_{\rm dc}$ (nm)	$d^S_{\rm cr}$ (nm)	$\rho(\mu\Omega$ cm)
1	2.0	0.1	0.42	28	6.3
0.88	1.74	0.3		32	70
0.77	1.57	0.2		35	69
0.53	1.0	0.2	0.86	34	168
0.38	0.39	0.3	1.44	30	94
0.34	0.25	0.4	2.06	28	92
0					10.6

multilayers, where the F metal is a ferromagnetic alloy with a moment which can be varied over almost an order of magnitude by changing the alloy composition. We determine $d^F_{\rm dc}$ and $d^S_{\rm cr}$ for different μ_F, and find a surprising nonmonotonic behavior for the latter. From analysis of the data using proximity effect theory, it is found that by including the interface transmission coefficient (or transparency) T as a parameter, we are able to account for the experimental results. We find that T strongly decreases with increasing μ_F. This may well be due to the spin splitting in the ferromagnet, which leads to partial reflection of Cooper pairs at the S/F interface as discussed for the conduction in Ref. 1.

II. EXPERIMENTAL

The multilayers were grown by dc magnetron sputtering as described previously.[9] They consist of V layers [T_c = 5.1 K, Ginzburg-Landau coherence length $\xi_{\rm GL}(0)$ = 13.9 nm] and $V_{1-x}Fe_x$ alloy layers. The case $x=1$ (V/Fe) was already studied.[10] In bulk V-Fe alloys, the average moment per Fe atom μ_F changes from $2.2\mu_B$ for pure Fe to 0 for $x=0.3$.[11] The main reason for choosing an alloy is to have different magnetic moments with the least changes of disorder at the interfaces. The V/Fe interface is well behaved, with a lattice mismatch of only 5% and with disorder confined to the two atomic planes on each side. The alloys have even smaller lattice mismatches with V, so that the favorable situation with respect to compositional disorder will remain.

Samples were grown with alloy compositions $x=1$, 0.88, 0.77, 0.53, 0.38, and 0.34. Three different sets of multilayers were prepared. One set was used to determine μ_F, built as follows: $d_V^{\rm out}$ / $N\times(d_V^{\rm in}/d_F)/d_V^{\rm out}$. The outer V layers $d_V^{\rm out}$ are for protection, typically 10–40 nm. The inner V layer $d_V^{\rm in}$ is typically 3 nm; it is not superconducting but meant to increase the number of interfaces, in order to obtain a realistic picture of the F layer magnetism. The F layer d_F is varied in thickness, typically between 0.5 and 5 nm, while the number of repetitions N is adapted to the strength of the moment. For Fe, $N=3$ suffices, while $N=20$ for $V_{66}Fe_{34}$. The magnetization M was measured with a magnetometer based on a superconducting quantum interference device at 5 or at 10 K. In all cases, M versus d_F could be described with a straight line, yielding the effective magnetic moment per Fe atom μ_F and the magnetically dead layer per interface $d_{\rm md}$ (see Ref. 9,10). They are given in Table I, while a comparison of

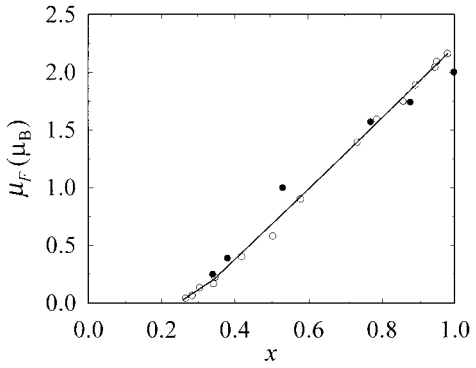

FIG. 1. The effective magnetic moment per Fe atom μ_F versus concentration x for alloys $V_{1-x}Fe_x$; ○ indicates bulk alloys, data taken from Ref. 11; ● indicates films, this work. The drawn line is meant to guide the eye.

$\mu_F(x)$ with values found in bulk alloys (from Ref. 11) is given in Fig. 1. Films and alloys show some differences; near $x=1$, the values in the films are slightly lower than in the bulk while below $x=0.75$ the films show higher values. We assume that this is due to the different morphologies of film and bulk material. Furthermore, $d_{\rm md}$ is relatively low in all cases. Values stay below about 0.3 nm or roughly one atomic layer, in clear contrast to the findings in the case of Co and Ni.[9]

The second sample set was used to determine $d^S_{\rm cr}$ by the variation of T_c as function of d_V. This is done with samples built with five layers (although three would suffice): $d_F/d_V/d_F/d_V/d_F$, with d_F fixed at around 5 nm (enough to represent a ''half-infinite'' layer) and d_V variable. The final set was used to determine $d^F_{\rm dc}$ by the variation of T_c with d_F; now five layers are needed: $d_F^{\rm out}/d_V/d_F^{\rm in}/d_V/d_F^{\rm out}$. The outer F layers are again of order 5 nm and meant to create a symmetric situation for the V layers when $d_F^{\rm in}$ is varied from 0 to 5 nm (essentially infinity); d_V has to be chosen differently for each alloy concentration which is best illustrated by some results.

III. RESULTS

Figure 2 shows a compilation of results for the alloy with $x=0.34$, having $\mu_F=0.25\mu_B$/(Fe atom), the smallest moment in the series. First we consider $T_c(d_V)$, shown in Fig. 2(a). The asymptotic value of 5.1 K for bulk V is reached above 150 nm. Below 50 nm, T_c starts to drop sharply, and $d^S_{\rm cr}$ is reached around 28 nm. Also shown are measurements of $d^F_{\rm dc}$. For this, d_V is chosen from the $T_c(d_V)$ curve, such that the single film T_c is in the range 2–3 K, well below the bulk value. This is then the measured T_c for the decoupling sample in the limit of large $d_F^{\rm in}$, called $T_c^{\rm low}$. Decreasing d_F leads to increasing T_c when the superconducting order parameters leaking out of the V layers start to overlap. At $d_F=0$, T_c reaches the value corresponding to 2 d_V in the $T_c(d_V)$ curve [dotted lines in Fig. 2(a)], which is called $T_c^{\rm high}$. In Fig. 2(b), such transition curves are shown for two different values of d_V, namely 40 and 55 nm. Both curves show a steep descent above 1 nm, and level off to values near $T_c^{\rm low}$ above 2 nm. Incidentally, neither curve shows an oscillation in T_c, as might be found if π coupling were

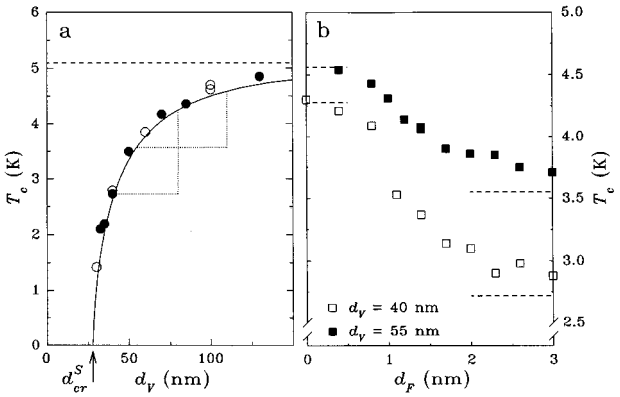

FIG. 2. Data for $V_{0.34}Fe_{0.66}$. (a) Critical temperature T_c versus V thickness d_V. Different symbols represent different sample sets. The dashed line shows the bulk T_c for V. The drawn line represents the model calculations, with γ and γ_b given in Table II. The dotted lines show the range of T_c values covered by the experiments displayed in (b). Also indicated is $d_{\rm cr}^S$. (b) T_c versus d_F for two values of d_V. The dashed lines show the limiting values as follow from the trilayer data in (a).

present. We will briefly come back to the issue of π coupling at the end of the Discussion.

In Fig. 3, the same transitions have been plotted, but scaled to $T_c^{\rm high}$-$T_c^{\rm low}$, and for all concentrations. For $x=0.34$ the curves for both thicknesses d_V essentially coincide, as they should. Furthermore, the steepest descent of the curves clearly shift to higher d_F upon decreasing x or μ_F. We now define $d_{\rm dc}^F$ by extrapolating the steepest slope in the transition curve to the d_F axis (see Fig. 3). Different definitions, such as using the 50% point, turned out to give very similar results. Values for $d_{\rm dc}^F$ are given in Table 1. We plot this quantity against μ_F^{-1} in Fig. 4 and find a reasonably linear relation. Making the identification $d_{\rm dc}^F/2=\xi_F$, it follows that ξ_F behaves as described by Eqs. (1,2). Given the small thicknesses involved, such clean-limit behavior could be expected, but the linear behavior also implies that the quantity $v_F/I_{\rm eff}$ basically remains constant with varying x.

Next we turn to the behavior of $d_{\rm cr}^S$. For all alloys, the

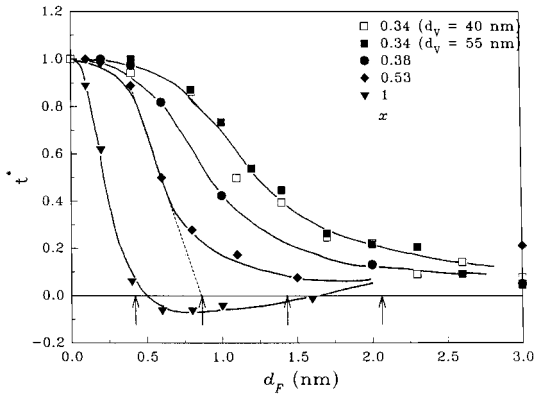

FIG. 3. Change of critical temperature T_c with F layer thickness d_F, scaled according to $t^*=(T_c-T_c^{\rm low})/(T_c^{\rm high}-T_c^{\rm low})$. The lines are meant to guide the eye. The construction for the determination of $d_{\rm dc}^F$ is indicated for $x=0.53$. The arrows show the values of $d_{\rm dc}^F$ for all alloy concentrations.

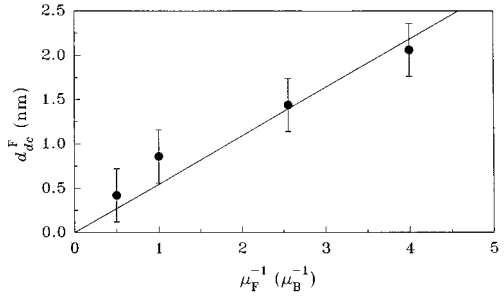

FIG. 4. Decoupling thickness $d_{\rm dc}$ versus inverse magnetic moment μ_F^{-1}. The line is a best fit through the data, and used to calculate ξ_F.

$T_c(d_V)$ curves are similar to the one presented in Fig. 2(a). The scatter in the individual points is small enough to find values for $d_{\rm cr}^S$ with good accuracy. All values for $d_{\rm cr}^S$ are collected in Table I. Especially interesting is the behavior near $x=1$, which is reproduced in Fig. 5. There, $T_c(d_V)$ is plotted on a somewhat expanded scale for the three systems with the highest moments ($x=1$, 0.88, 0.77). The behavior for $x=1$, 0.77 is very smooth; for $x=0.88$, the scatter in points is quite large, actually the largest by far of all sets measured [compare also Fig. 2(a) for $x=0.34$]. Even then, the plot unequivocally shows that the curves shift to higher thickness with decreasing x. This behavior is quite unexpected, and comprises the main issue of our research, to be discussed below. Figure 6 shows the full behavior of $d_{\rm cr}^S(\mu_F)$. A clear maximum is found between $x=0.77$ and $x=0.53$, before a slow decrease sets in. The value at $x=0.34$, where the magnetic moment has decreased by a factor 8, is actually equal to the value for $x=1$ (Fe). To make the point in another way, we plotted in Fig. 6 the results of earlier measurements with Co and Ni as the F metal (open circles),[9] where $d_{\rm cr}^S$ is found to be much lower at the same values for the magnetic moment. Next to μ_F, another factor must play a major role in determining the physics. We will now argue that this factor is the interface transparency.

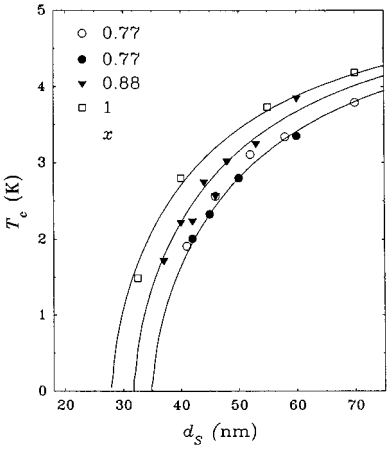

FIG. 5. Change of critical temperature T_c with S layer thickness d_S for alloys with $x=1$, 0.88, and 0.77 (two sample sets). The lines are the results of the calculations with the parameters given in Table II.

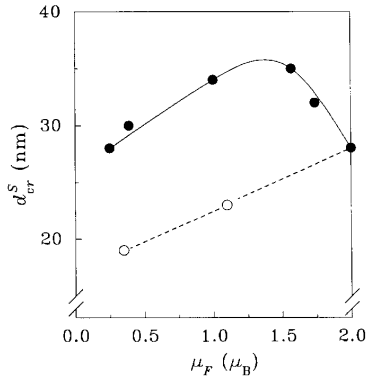

FIG. 6. ● indicates values of the critical thickness $d_{\rm cr}^S$ for all alloy concentrations plotted versus magnetic moment μ_F. ○ indicates data for Co and Ni taken from Ref. 9. Drawn and dashed lines are meant to guide the eye.

IV. DATA ANALYSIS BY PROXIMITY EFFECT THEORY

A. Theory; a brief description

Scattering of a normal electron or quasiparticle on a potential barrier at an interface will lower its transmission coefficient T. In S/N structures, one source for this is the potential step due to the difference in lower band-edge energies. Defects can also cause potential scattering, and are usually modeled as a δ function with a certain strength. Theoretically, the consequences of reduced T for different quantities such as the superconducting density of states or the critical temperature, have long been a subject for investigation, starting with McMillan's tunneling model for bilayers, which represents the limit of small T. A good overview of the early work can be found in Ref. 12. Experimentally, T is usually treated as an adjustable parameter. Systematic investigations have been few, as are numbers for the ''intrinsic'' value of T in a given NS combination. This may not be surprising, since interface imperfections play an important role. It is also useful to remark that the transparency discussed here is conceptually equal to the barrier strength parameter Z in the Blonder-Tinkham-Klapwijk model[13] for transport properties of tunnel junctions.

Recently, model calculations were performed on the proximity effect in S/N multilayers for arbitrary transparency of the interface.[14] The model is based on the Usadel equations, with boundary conditions for the normal and anomalous Green's functions at the interface as derived by Kuprianov and Lukichev,[15] following earlier work on the clean-limit case by Zaitsev.[16] The model can be easily adapted to the S/F case by noting that the coherence length in the F metal is determined by $\Delta E_{\rm ex}$ and therefore independent of temperature.[4–6] In an earlier analysis of results on V/Fe multilayers[9,10] a similar model was used (due to Radović *et al.*[4]), which could well describe the behavior of critical temperatures and critical fields, but did not incorporate interface transparency explicitly. As a matter of fact, the single parameter ϵ of that model is, in general, not suited to describe proximity effect and transparency in an independent way, although it turns out to be possible in the limiting case of F/S/F trilayers with $d_F \gg \xi_F$. This point is quite important for the correct description of experimental results and therefore the model and this issue in particular will be discussed

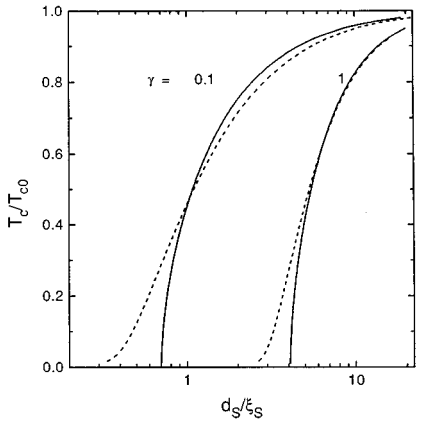

FIG. 7. The calculated change in relative critical temperature T_c/T_{c0} with changing S layer thickness d_S/ξ_S for an F/S/F trilayer (drawn lines) and an N/S/N trilayer (dashed lines), for $\gamma=0.1$, 1 and complete transparency ($\gamma_b=0$).

in the Appendix. Here, we continue with showing some of the results of the model calculations, which will serve to illustrate the analysis of the experiments. For the underlying data, we need the dependence $T_c(d_S)$, for different values of the proximity effect parameter γ and the transparency parameter γ_b, defined as (see the Appendix):

$$\gamma=\frac{\rho_S\xi_S}{\rho_F\xi_F}, \quad \gamma_b=\frac{R_B}{\rho_F\xi_F}, \tag{3}$$

with ρ_i the normal-state resistivity of metal i, and R_B the normal-state boundary resistance times its area. The connection between γ_b and the transparency T is roughly given by

$$T=\frac{1}{1+\gamma_b}. \tag{4}$$

Figures 7 and 8 show two types of results from the calculations. In Fig. 7, $T_c(d_S)$ is given for an F/S/F trilayer with $d_F=10\xi_F$, $\rho_S=\rho_F$, $\xi_S/\xi_F=10$ ($\gamma=10$) and complete trans-

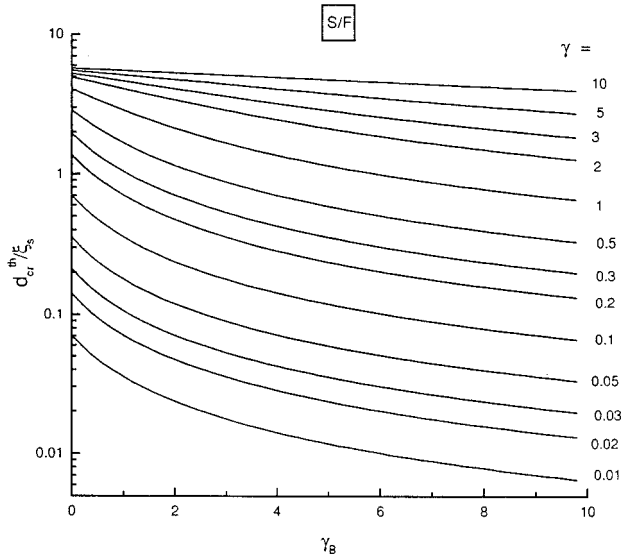

FIG. 8. The calculated change in critical thickness $d_{\rm cr}^{\rm th}/\xi_S$ for an F/S/F trilayer as function of the transparency parameter γ_b for different values of the proximity effect parameter γ.

TABLE II. Values for the coherence lengths ξ_F, for the specific resistivity ρ at 6 K, for the proximity-effect parameter γ, and for the transparency parameter γ_b, for alloys $V_{1-x}Fe_x$.

x	ξ_F (nm)	$\rho(\mu\Omega$ cm)	γ	γ_b
1	0.14	6.3	109	180
0.88	0.16	70	8.5	10.1
0.77	0.17	69	7.8	7.3
0.53	0.27	168	2.1	1.3
0.38	0.69	94	1.4	1.1
0.34	1.08	92	0.93	0.6
0		10.6		

parency ($\gamma_b=0$), and an N/S/N trilayer with the same parameters. The difference between both curves is quite small and only clearly visible below $T_c/T_{c0}\approx 0.5$, where the temperature dependence of ξ_N becomes important. In the F case, it is easy to define a value for the critical thickness, called $d_{\rm cr}^{\rm th}$, for which we take the thickness at $T_c/T_{c0} = 0.01$. Figure 8 shows the behavior of $d_{\rm cr}^{\rm th}$ for the F/S/F case as function of the parameters γ and γ_b. The plot demonstrates some general features of proximity effect systems. In the large-γ limit, $d_{\rm cr}^{\rm th}/\xi_S \rightarrow \pi\sqrt{2\gamma_E} \approx 6$, with γ_E the Euler constant. This limit is hard to reach in S/N systems, where ξ_S, ξ_N are of the same order of magnitude, but is easily met in S/F systems with ρ_S/ρ_F of order one, and with ξ_S an order of magnitude larger than ξ_F. Also, if γ is large and therefore ''proximity leak'' is small, it takes a very high barrier (large γ_b, small T) to lower $d_{\rm cr}^{\rm th}$.

B. Discussion of the results

As has been discussed above, a full description of the T_c variation in a proximity effect system needs five parameters: the S bulk layer critical temperature T_{c0}, the thicknesses d_S and d_F, the proximity-effect strength γ and the transparency parameter γ_b. Starting with γ, it can be seen from Eq. (3) that this parameter is fully determined by measurable quantities. We take ξ_F from the linear relation between $d_{\rm dc}^F$ and μ_F^{-1}, shown in Fig. 3, rather than from the actual values of $d_{\rm dc}^F$. The values used are given in Table II. For ξ_S we use 8.8 nm, corresponding to $\xi_{\rm GL}(0) = 13.9$ nm.[10] The normal-state resistivities $\rho_{S,F}$ are also known. They were measured on thin films of 50, 100, and 200 nm, down to 6 K for all compositions and for V. The averaged values are given in Table II. Due to the use of alloys, ρ_F actually increases considerably (about 2 $\mu\Omega$ cm/at %) up to $x=0.5$, thereby lowering the resistivity ratio in γ from 1.7 to 0.06. Values for γ can now be calculated, and they are found (see Table II) to decrease monotonically with decreasing moment. Note that this is due to a decrease in both the factors ρ_S/ρ_F and ξ_S/ξ_F, and neither factor therefore can be the cause of the measured increase of $d_{\rm cr}^S$. With the values for γ, we calculate theoretical values $d_{\rm cr}^{\rm th}$ under the assumption that $\gamma_b = 0$. The numbers, plotted as squares in Fig. 9(a), do not mimick the experimental results, shown as filled circles, in two respects. They do not go through a maximum, as was already anticipated from the monotonic behavior of γ, but also, the measured values are much lower than the calculated

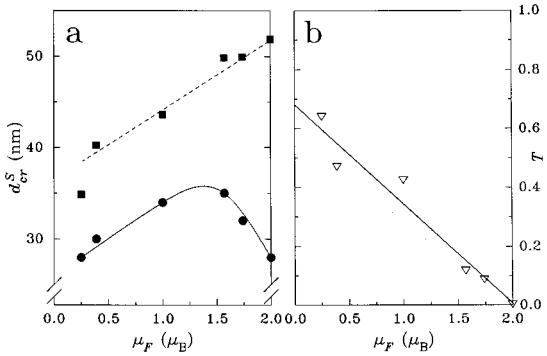

FIG. 9. (a) (●) indicates Critical thickness $d_{\rm cr}^S$ versus magnetic moment μ_F for all alloy concentrations; (■) indicates calculated critical thickness $d_{\rm cr}^{\rm th}$, computed with $\gamma_b = 0$ (full transparancy). (b) transparency T versus alloy magnetic moment μ_F. All lines are meant to guide the eye.

ones. Especially for Fe, a low value for ξ_F and an also relatively low value for ρ_F lead to a very high γ and a theoretical critical thickness which is close to the asymptotic limit of about 6 ξ_S.

The simple fact that $d_{\rm cr}^S$ is much smaller than expected for the case $\gamma_b=0$, already indicates reduced interface transparency; a value for $T<1$ ($\gamma_b>0$) leads to smaller $d_{\rm cr}^S$ (see Fig. 8); for $T=0$ the superconductor will behave as an isolated film ($d_{\rm cr}\rightarrow 0$). The next step therefore is to use the model calculations in order to find the value of γ_b needed to reproduce the measured values for $d_{\rm cr}^S$. T is then simply found from Eq. (4). The results, plotted in Fig. 9(b), show a very simple relation: T is low for the case of Fe, increases more or less linearly with decreasing μ_F or x, and reaches the order of 1 for low Fe concentration. The observed maximum in $d_{\rm cr}^S$ is therefore due to the competition of three ingredients: on the side of high Fe concentration, the increasing ξ_F and decreasing ρ_S/ρ_F will lower $d_{\rm cr}^S$, but the increasing interface transparency will increase $d_{\rm cr}^S$, and wins; on the low Fe side, the change in interface transparency has become less important, and the change in $d_{\rm cr}^S$ is as expected from the change in γ.

We believe this to be the first demonstration of a barrier transparency which is changed in a continuous (and controlled) fashion, and over a large part of the full range. Of course, the given values for T should not be taken too literally. They depend on the way in which ξ_F is extracted from the $T_c(d_F)$ curves, on the measured values of $\rho_{S,F}$ (which may be somewhat different in multilayers or in single films), and on the approximation used to go from γ_b to T. Especially a near-zero value for Fe may be too low. On the other hand, a seriously reduced T is needed to explain the low value for $d_{\rm cr}^S$, while a serious concentration or moment dependence of T is needed to explain the increase in $d_{\rm cr}^S$. This point leads to the question of the cause of the low value and its change. It is possible that T depends on x as a result of the changing compositional disorder or the changing lattice parameters (strain). It is more probable, however, that μ_F, meaning the ferromagnetism and the spin-dependent band structure, play a role. One mechanism may well be the reduction of Andreev scattering due to the exchange splitting,[1]

since this would translate to a reduced transparency through the use of the boundary conditions for the Usadel equations (see the Appendix). The effect is linear in $\Delta E_{\rm ex}/\epsilon_F$, with ϵ_F the Fermi energy, and might therefore be appreciable, of the order of 30–50 %. Another mechanism can be spin dependence in the normal-state reflection at the interface, such as now investigated in view of giant magnetoresistance effects (see, e.g., Ref. 17). It would take reflections in only one spin channel to lower the transparency for Cooper pairs. Both effects can be present at the same time; from this viewpoint, low transparency looks quite feasible. Interestingly, the few reported values for $d_{\rm cr}^S/\xi_S$ are much below the upper limit of 6. For Nb/Gd, for instance, the value is 4.2.[18] For Nb/Er, the value appears to be between 2 and 3.[19] Low transparency may prove to be a general phenomenon in S/F multilayers.

C. On the issue of π coupling

In the discussion of the results on the decoupling behavior, we already noted that no oscillatory behavior of T_c, and therefore no indication of π coupling is found with varying thickness of the magnetic layer for any alloy concentration or magnetic moment. This may not be very surprising. In the original description[3] of a possible mechanism which changes the phase of a Cooper pair by π, the transfer of the pair through a barrier containing localized moments is accompanied by two virtual spin flips of that moment. Given the strong and itinerant nature of the magnetism in the $3d$ transition metals under consideration, the spin flips would take the form of spin-wave excitations. This process will have a small probability in view of the large energy denominator involved. In principle, a system with strongly localized (e.g., $4f$) moments, might offer a better chance for finding π coupling. Still, we do not believe that the oscillationlike changes in T_c which were found recently in Nb/Gd (Ref. 7) are actually due to this mechanism. Rather, transparency may again play an important role, as can also be inferred from a report on oscillatory T_c's in Nb/Fe by Mühge *et al.*,[8] who investigated (essentially) trilayer samples with a single superconducting layer. The key observation in both Nb/Gd and Nb/Fe is that T_c increases *at the onset* of ferromagnetism in the thin F layer. In the spirit of the model used above, we would describe this in the following way: at thicknesses below the onset, strong paramagnetic fluctuations will still act as pair breakers of a strength comparable to the one in the ferromagnet and T_c goes down with increasing d_F. At the onset, a static exchange splitting sets in, decreasing the interface transparency and *increasing* T_c. Since this jump will be superimposed on a falling $T_c(d_F)$ curve, it is entirely feasible that T_c decreases again with further increase of d_F. Also, the fact that these very thin films have not yet reached their bulk Curie temperature will still change ξ_F and $\Delta E_{\rm ex}$ beyond the transition to ferromagnetism. It is interesting to speculate that in the results on Nb/Gd reported by Strunk *et al.*,[18] the onset of ferromagnetism occurs where the plateau in $T_c(d_{\rm Gd})$ begins, rather than at the downward jump. The reason that no clear plateaulike effects are seen in the measurements presented here is then that for the Fe-rich alloys magnetism already sets in at very small d_F where the resolution is poor, whereas on the dilute side the transparency change has become small, with a correspondingly small effect on T_c.

V. SUMMARY

In summary, we investigated decoupling in S/F/S structures upon varying the magnetic moment of the F layer atoms. Indications of π coupling in the form of T_c oscillations are not observed. Identifying $d_{\rm dc}^F$ with ξ_F we find a simple and reasonable dependence $\xi_F \propto \mu_F^{-1}$. We also measured the critical thickness $d_{\rm cr}^S$ in F/S/F structures. Here we find a surprising and nonmonotonous behavior as function of μ_F. By analyzing the data in terms of a proximity effect theory, we conclude that this behavior is due to the competing effects of increasing attenuation depth (ξ_F) of the order parameter in the F material, and of also increasing transparency of the S/F interface for the penetration of Cooper pairs. More insight in this effect should come from a better understanding of the spin dependence of the different scattering mechanisms at the interface.

ACKNOWLEDGMENTS

We would like to thank P. Koorevaar for early contributions to this work, and J.A. Mydosh, P.H. Kes, and C.J.M. Beenakker for discussions. This work is part of the research program of the ''Stichting voor Fundamenteel Onderzoek der Materie'' (FOM), which is financially supported by NWO.

APPENDIX

We consider a multilayered structure consisting of alternating F and S layers of thickness d_F and d_S, respectively, and with a finite transparency of the FS boundary. The S layer has a bulk critical temperature T_{c0}. We assume dirty-limit conditions for both F and S metals: $l_{F,S} \ll \xi_{F,S}$, where $l_{F,S}$ and $\xi_{F,S}$ are the mean free paths and coherence lengths in the F(S) layers. Due to the translational symmetry of the problem it is sufficient to consider an elementary unit cell with period $\Lambda=(d_F+d_S)/2$. With these assumptions the proximity effect in the system can be described within the framework of the Usadel equations for the S and F layers. Near T_c these equations can be linearized and written in the form[5,6]

$$\xi_S^2 \frac{\pi T_c}{|\omega|} \frac{d^2}{dx^2}\Phi_S^{\pm} - \Phi_S^{\pm} = 2\Delta\,\delta^{\pm}, \quad 0<x<d_S, \tag{A1}$$

$$\xi_F^2 \frac{d^2}{dx^2}\Phi_F^{\pm} \mp i\Phi_F^{\mp} = 0, \quad -d_F<x<0, \tag{A2}$$

$$\Delta \ln\frac{T_c}{T_{c0}} + \pi T_c \sum_{\omega>0} [(2\Delta - \Phi_S^{+})/\omega] = 0. \tag{A3}$$

Here $\Phi_{F,S}^{\pm} \equiv \Phi_{F,S}(\omega) \pm \Phi_{F,S}(-\omega)$ are the anomalous Green's functions integrated over energy and averaged over the Fermi surface, Δ is the order parameter in the S layer, $\delta^+=1$, $\delta^-=0$, and $\omega=\pi T(2n+1)$ with $n=0,\pm1,\pm2,\ldots$ are the Matsubara frequencies. Note that the functions

$\Phi_{F,S}(\omega)$ are not symmetric with respect to sign reversal of the energy ω, i.e., $\Phi_{F,S}(\omega)\neq\Phi_{F,S}(-\omega)$. This symmetry is restored in the more conventional case of proximity effect in an NS sandwich: $\Phi_{N,S}(\omega)=\Phi_{N,S}(-\omega)$, which results in $\Phi^{+}_{N,S}\equiv 2\Phi_{N,S}$, and $\Phi^{-}_{N,S}=0$. Another important difference between the NS and FS cases is that ξ_N is ω dependent, whereas ξ_F is constant. Some specific phenomena which result from these peculiarities of FS systems were pointed out previously in Refs. 4–6. Here we are interested in the effects of the intransparency of an FS interface. Similar to the case of an NS sandwich, Eqs. (A1) and (A2) must be supplemented with the following boundary conditions in the middle of the layers:

$$\frac{d}{dx}\Phi^{\pm}_{S}(x=d_S/2)=0, \quad \frac{d}{dx}\Phi^{\pm}_{F}(x=-d_F/2)=0, \quad \text{(A4)}$$

as well as at the FS boundary[15]

$$\xi_S\frac{d}{dx}\Phi^{\pm}_{S}=\gamma\xi_F\frac{d}{dx}\Phi^{\pm}_{F}, \qquad \xi_F\gamma_b\frac{d}{dx}\Phi^{\pm}_{F}=\Phi^{\pm}_{S}-\Phi^{\pm}_{F}, \quad \text{(A5)}$$

where

$$\gamma=\frac{\rho_S\xi_S}{\rho_F\xi_F}, \quad \gamma_b=\frac{R_B}{\rho_F\xi_F}. \quad \text{(A6)}$$

Here ξ_F is defined in Eq. (1), ξ_S is defined as $\xi_S=2\xi_{\mathrm{GL}}(0)/\pi$, ρ_i is the normal-state resistivity of metal i, and R_B is the normal-state boundary resistance times its area. Equation (A3) is a self-consistency equation for the order parameter in the S layer. The parameters γ and γ_b have a simple physical meaning: γ is a measure of the strength of the proximity effect between the F and S metals, whereas γ_b, given by

$$\gamma_b=(2/3)(l_F/\xi_F)\langle(1-T(\theta))/T(\theta)\rangle \quad \text{(A7)}$$

describes the effect of the boundary transparency. The parameter $T(\theta)$ denotes the transmission coefficient through the interface for a given angle θ between the quasiparticle trajectory and interface and $\langle\ldots\rangle$ denotes the angle averaging over the Fermi surface. The condition $\gamma_b=0$ corresponds to a perfectly transparent boundary, whereas $\gamma_b=\infty$ corresponds to a vanishingly small boundary transparency. Specific expressions for T can be obtained for certain models for the potential barrier. The case of a δ-potential barrier $U(x)=U_0\delta(x-x_0)$ yields $T(\theta)=4v_F(\theta)v_S(\theta)/\{4U_0^2+[v_F(\theta)+v_S(\theta)]^2\}$, where $v_{F,S}(\theta)$ are the projections of the Fermi velocities of F and S metals on the direction perpendicular to the interface. If the exchange splitting in the ferromagnet is the main cause for intransparency, a simple expression for T was given in Ref. 1. By assuming a Stoner-like model, in which the exchange energy h_0 results in a potential step for one of the spin subbands, it follows that

$$T_{\mathrm{SF}}(\theta)=\frac{4k_S^2k_\uparrow k_\downarrow}{(k_S^2+k_\uparrow k_\downarrow)^2}, \quad \text{(A8)}$$

where the different wave vectors must be projected on the direction perpendicular to the interface, giving the θ dependence. For equal and free-electron-like bands: $k_S\propto\sqrt{\epsilon}$, $k_\uparrow\propto\sqrt{\epsilon-h_0}$, $k_\downarrow\propto\sqrt{\epsilon+h_0}$, with ϵ the energy of the electron with respect to the Fermi energy, it can easily be shown that $T=1$ when $h_0=0$, while $T=0$ for $h_0=\epsilon_F$, since then no occupied states are present for the $k_\uparrow$ subband. In between these limits, $T(h_0)$ is roughly linear.[1]

Equations (A1) and (A2) were discussed extensively in Refs. 20,21 in connection with the proximity effect in NS sandwiches with thick S layers and thin N layers, which is a particular case of the multilayer problem. It was shown there that solving Eqs. (A1) and (A2) may be reduced to solving Eqs. (A1) and (A3) in the S region with an effective boundary condition for $\Phi_S(0)$. Such a boundary condition can be derived for certain limits. For instance, solving the equation for Φ_N in the N region and using the boundary conditions of Eq. (A5) in the linear regime under consideration near T_c, one obtains

$$\Phi'_S(0)=\frac{\gamma A_N(\omega)}{1+\gamma_b A_N(\omega)}\Phi_S(0), \quad \text{(A9)}$$

where the parameter $A_N(\omega)$ is given by the expression

$$A_N(\omega)=\left(\frac{\omega}{\pi T_{c0}}\right)^{1/2}\tanh\left[\left(\frac{d_N}{2\xi_N}\right)\left(\frac{\omega}{\pi T_{c0}}\right)^{1/2}\right], \quad \text{(A10)}$$

with $\xi_N=\sqrt{v_N l_N/6\pi T_{c0}}$.

In the case of an FS sandwich, one needs an effective boundary condition for Φ^{+}_S, since this function goes into the self-consistency equation (A3). Such a boundary condition was derived in Refs. 5,6 for the case of a fully transparent FS interface and may be straightforwardly generalized for the case of arbitrary transparency using Eq. (A5). The condition is simplified considerably in the most interesting case of a large exchange splitting ΔE_F; one arrives at an expression similar to Eq. (A9) with A_N substituted by A_F. The length ξ_F is independent of temperature, which means that $A_F(\omega)$ becomes independent of ω:

$$A_F=\left[\sin^2\left(\frac{d_F}{2\xi_F}\right)\tanh\left(\frac{d_F}{2\xi_F}\right)+\cos^2\left(\frac{d_F}{2\xi_F}\right)\coth\left(\frac{d_F}{2\xi_F}\right)\right]^{-1}. \quad \text{(A11)}$$

Relation (A11) leads to the oscillatory dependence of T_c on F layer thickness discussed theoretically in Refs. 4–6. Furthermore, $A_F=1$ in the limit of thick F layers, $d_F/2\xi_F\gg 1$. As a result, in the latter regime the effective parameter in the boundary condition [Eq. (A9)] becomes $\gamma/(1+\gamma_b)$, i.e., the transparency can be incorporated in a single parameter. It is then possible to find the correspondence between this single parameter and the parameter ϵ from the model of Radović *et al.*,[4] defined as

$$\epsilon=\frac{\xi_S}{\eta\xi_F}. \quad \text{(A12)}$$

Simple algebraic manipulation shows that, since for full transparency we have $\gamma=\epsilon^{-1}$, for arbitrary transparency we must have

$$\eta = \frac{\rho_S}{\rho_F}\frac{1}{1+\gamma_b}. \tag{A13}$$

In this same case of thick F layers, the equations for T_c also reduce to a very simple form:

$$\Omega \tan(\Omega d_S/2\xi_S) = \gamma/(1+\gamma_b),$$
$$\psi(1/2+\Omega^2 T_{c0}/2T_c) - \psi(1/2) = \ln(T_{c0}/T_c). \tag{A14}$$

It is interesting to note that these equations are nothing else than those from the de Gennes–Werthamer theory,[22,23] with the effective boundary condition introduced above. Furthermore, it should be remarked that the single parameter description only holds for the linear problem near T_c whereas the behavior of the densities of states in S layers is not simply scaled as $\gamma/(1+\gamma_b)$.

Finally, it is easy to solve Eqs. (A14) in two limiting cases of weak and strong suppression of T_c. In the first regime, where $(T_{c0}-T_c)/T_{c0} \ll 1$, the thickness dependence of T_c has the form:

$$T_c/T_{c0} \simeq 1 - \frac{\pi^2 \xi_S}{2d_S}\frac{\gamma}{1+\gamma_b}, \quad \gamma/(1+\gamma_b) \ll 1, \tag{A15}$$
$$T_c/T_{c0} \simeq 1 - \left(\frac{\pi^2 \xi_S}{2d_S}\right)^2, \quad \gamma/(1+\gamma_b) \gg 1.$$

The critical thickness $d_{\rm cr}^{\rm th}$ is easily found by taking the limit $T_{c0}/T_c \to \infty$ and using the asymptotic form $\psi(z) \simeq \ln(4\gamma_E z)$ at $z \gg 1$ in the second part of Eq. (A14) (where $\gamma_E \simeq 1.78$ is the Euler constant). We obtain $\Omega_{\rm cr}^2 = 1/2\gamma_E$ and then the first part of Eq. (A14) yields $d_{\rm cr}^{\rm th,SF}/\xi_S = \pi\sqrt{2\gamma_E} \simeq 5.93$ for $\gamma/(1+\gamma_b) \gg 1$, and $d_{\rm cr}^{\rm th,SF}/\xi_S = 4\gamma_E\gamma/(1+\gamma_b)$ for $\gamma/(1+\gamma_b) \ll 1$.

The well known de Gennes result for the critical thickness for SN systems with full transparency, $\gamma_b = 0$, and $\gamma \ll 1$ reads $d_{\rm cr}^{\rm th,SN}/\xi_S = 2\sqrt{2\gamma_E\gamma}$.[24] Thus, for comparable values of the pair-breaking parameter γ the critical thickness in an SN multilayer is somewhat smaller than in an SF one. A comparison of $T_c(d_s/\xi_S)$ curves for SF and SN multilayers was already made in Fig. 7 for two values of γ and for $\gamma_b = 0$. In accordance with earlier calculations (see Ref. 4 and references therein) the behavior of $T_c(d_s/\xi_S)$ for SF and SN is most different in the regime of strong pair breaking, $T_c/T_{c0} \ll 1$, where the drop of T_c in the SF case is steeper. Nevertheless, a critical thickness exists both in the SF and SN cases; it is a general property of proximity-effect systems, provided that the N(F) layers are thick. To illlustrate this, in Fig. 10 we compare the dependences of $d_{\rm cr}^{\rm th}/\xi_S$ on the interface transparency in the S/F and S/N cases for several values of γ. In both cases, $d_{\rm cr}^{\rm th}$ was taken at the value where $T_c/T_{c0} \ll 0.01$. Since $d_{\rm cr}^{\rm th}$ is controlled by the parameter $\gamma/(1+\gamma_b)$, it decreases with the increase of the intransparency parameter γ_b and with the decrease of the pair-breaking parameter γ. The curves in Fig. 10 may be used to estimate critical thicknesses in real multilayer structures.

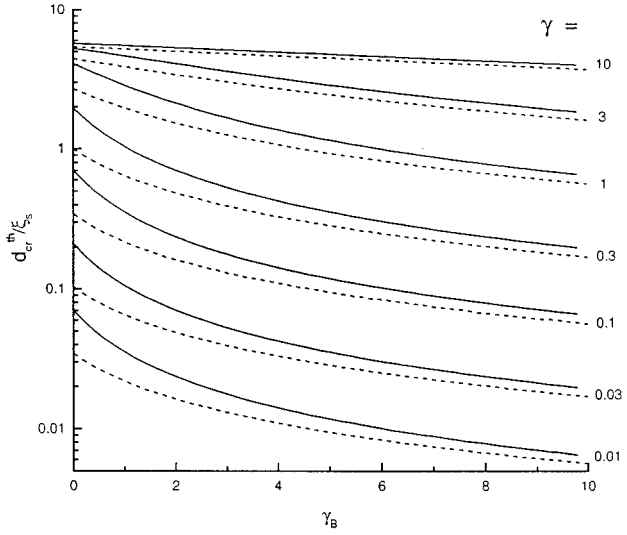

FIG. 10. Comparison of the calculated change in critical thickness $d_{\rm cr}^{\rm th}/\xi_S$ for F/S/F trilayers (drawn lines) and N/S/N trilayers (dashed lines) as function of the transparency parameter γ_b for different values of the proximity-effect parameter γ.

*Present address: Dept. of Applied Physics, University of Twente, P.O. Box 217, 7500 AE Enschede, the Netherlands.

[1] M.J.M de Jong and C.W.J. Beenakker, Phys. Rev. Lett. **74**, 1657 (1995).
[2] H. Pothier, S. Guéron, D. Esteve, and M.H. Devoret, Phys. Rev. Lett. **73**, 2488 (1995).
[3] L.N. Bulaevskiĭ, V.V. Kuziĭ, and A.A. Sobyanin, JETP Lett. **25**, 290 (1977).
[4] Z. Radović, M. Ledvij, L. Dobrosavljević-Grujić, A.I. Buzdin, and J.R. Clem, Phys. Rev. B **44**, 759 (1991).
[5] A.I. Buzdin and M.Yu. Kupriyanov, JETP Lett. **52**, 487 (1990).
[6] A.I. Buzdin, B. Bujicic, and M.Yu. Kupriyanov, Sov. Phys. JETP **74**, 124 (1992).
[7] J.S. Jiang, D. Davidović, D.H. Reich, and C.L. Chien, Phys. Rev. Lett. **74**, 314 (1995).
[8] Th. Mühge, N.N. Garif'yanov, Yu.V. Goryunov, G.G. Khaliullin, L.R. Tagirov, K. Westerholt, I.A. Garifullin, and H. Zabel, Phys. Rev. Lett. **77**, 1857 (1996).
[9] P. Koorevaar, R. Coehoorn, and J. Aarts, Physica C **248**, 61 (1995).
[10] P. Koorevaar, Y. Suzuki, R. Coehoorn, and J. Aarts, Phys. Rev. B **49**, 441 (1994).
[11] K. Adachi, in *Magnetic Properties of Metals*, edited by H.P.H. Wijn, Landolt-Börnstein, New Series Vol. III-19a (Springer, Berlin, 1986).
[12] E.L. Wolf, *Principles of Electron Tunneling Spectroscopy* (Oxford University Press, Oxford, 1985).
[13] G.E. Blonder, M. Tinkham, and T.M. Klapwijk, Phys. Rev. B **25**, 4515 (1982). See also G.E. Blonder and M. Tinkham, *ibid.* **27**, 112 (1983), for a discussion of the effects of Fermi velocity differences on Z.
[14] A.A. Golubov, Proc. SPIE **2157**, 353 (1994).
[15] M.Yu. Kuprianov and V.F. Lukichev, Sov. Phys. JETP **67**, 1163 (1988).
[16] A.V. Zaitsev, Sov. Phys. JETP **59**, 1015 (1984).

[17] K.M. Schep, P.J. Kelly, and G.W. Bauer, Phys. Rev. Lett. **74**, 586 (1995).
[18] C. Strunk, C. Sürgers, U. Paschen, and H. v. Löhneisen, Phys. Rev. B **49**, 4053 (1994).
[19] L.H. Greene, W.H. Feldmann, J.M. Rowell, B. Batlogg, E.M. Gyorgy, W.P. Lowe, and D.B. McWhan, Superlattices Microstruct. **1**, 407 (1985).
[20] A.A. Golubov and M.Yu. Kupriyanov, Sov. Phys. JETP **69**, 805 (1989).
[21] A.A. Golubov, M.A. Gurvich, M.Yu. Kupriyanov, and S.V. Polonskii, Sov. Phys. JETP **76**, 915 (1993).
[22] P.G. de Gennes and E. Guyon, Phys. Lett. **3**, 168 (1963).
[23] N.R. Werthamer, Phys. Rev. **132**, 2440 (1963).
[24] P.G. de Gennes, Rev. Mod. Phys. **36**, 225 (1964).